Elastic scattering of 10 MeV ^{6}He from ^{12}C, ^{nat}Ni, and ^{197}Au

R. E. Warner,* F. D. Becchetti, J. W. Jänecke, and D. A. Roberts
Department of Physics, University of Michigan, Ann Arbor, Michigan 48109

D. Butts, C. L. Carpenter, J. M. Fetter,† and A. Muthukrishnan
Physics Department, Oberlin College, Oberlin, Ohio 44074

J. J. Kolata, K. Lamkin, M. Belbot, and M. Zahar
Physics Department, University of Notre Dame, Notre Dame, Indiana 46556

A. Galonsky, K. Ieki,‡ and P. Zecher
Department of Physics and National Superconducting Cyclotron Laboratory, Michigan State University, East Lansing, Michigan 48824

(Received 17 June 1994)

A radioactive nuclear beam of 10.2 MeV ^{6}He, with typical intensity 5×10^4 s^{-1}, was produced via the ^{9}Be(^{7}Li,^{6}He)^{10}B reaction and elastically scattered from targets of ^{12}C, ^{nat}Ni, and ^{197}Au. Scattering from C and Ni was observed through sufficiently large angles (up to 60° c.m. and 85° c.m., respectively) to show large deviations from Rutherford scattering. The Au target gave, as expected, pure Rutherford scattering. Optical potentials previously used for low-energy ^{6}Li and ^{8}Li ions generally accounted for the shapes of the angular distributions but, for ^{12}C, predict oscillations not present in the ^{6}He data. ^{4}He optical potentials predict much smaller deviations from Rutherford scattering than those observed.

PACS number(s): 25.70.Bc, 25.60.+v, 24.10.Ht, 27.20.+n

I. INTRODUCTION

Elastic scattering is a traditional method of finding the interaction between two nuclei; most often, a Woods-Saxon optical-model potential (OMP) is used to describe the interaction. The availability of radioactive nuclear beams (RNB's) can now give us new information on whether the potential parameters vary systematically with N and Z. For instance, Moon *et al.* [1] used very similar OMP's to fit the scattering of 60 MeV/nucleon ^{6}Li, ^{7}Li, and ^{9}Li on protons, but their ^{11}Li data required a more shallow real potential and an imaginary potential with a longer tail, presumably reflecting the halo property of ^{11}Li. Becchetti *et al.* [2] found satisfactory OMP's for 14-MeV ^{8}Li on nuclei from ^{9}Be to ^{58}Ni which differed only in their imaginary potential depths, and which also fitted published ^{6}Li and ^{7}Li elastic-scattering data.

^{6}He is an interesting nucleus because of both its participation in the helium-burning reaction chains in nucleosynthesis and its neutron halo whose measured [3] thickness, 0.9 fm, agrees with realistic microscopic multicluster calculations [4]. Little is known about the ^{6}He OMP; however, since it has many low-$|Q|$ reaction channels, its behavior may therefore resemble that of ^{4}He less closely than that of the light Li isotopes. Only one elastic-scattering study, that of Smith *et al.* [5], has been reported at low energies. They bombarded targets from ^{9}Be to ^{197}Au with 8- and 9-MeV ^{6}He. Deviations from Rutherford scattering were observed only for Be and C, which were measured only for laboratory angles less than 35° and 30°, respectively.

Our present measurements of 10-MeV ^{6}He elastic scattering on ^{12}C, ^{nat}Ni, and ^{197}Au extend the work of Smith *et al.* [5]; data are obtained for sufficiently large angles to show large deviations from Rutherford scattering for both C and Ni. We compare the data with optical-model predictions using parameters originally obtained from ^{4}He, ^{6}Li, and ^{8}Li scattering data.

II. EXPERIMENTAL PROCEDURE AND RESULTS

Our radioactive nuclear beam facility, the University of Michigan 3.5-T superconducting solenoid installed at the University of Notre Dame tandem van de Graaff accelerator, has been described in detail elsewhere [6,7]. The present measurements utilized the ^{9}Be(^{7}Li,^{6}He)^{10}Be production reaction, initiated by a 16.0-MeV ^{7}Li primary beam on a 12.7-μm ^{9}Be target. A ^{6}He beam of average energy 10.2 MeV, with 0.8-MeV FWHM and typical intensity 5×10^4 s^{-1}, was focused by the solenoid on secondary targets 2.1 m further downstream. The ^{6}He

*Permanent address: Physics Department, Oberlin College, Oberlin, OH 44074.

†Present address: Physics Department, University of Wisconsin, Madison, WI 53706.

‡Permanent address: Department of Physics, Rikkyo University, 3 Nishi-Ikebukuro, Toshima, Tokyo 171, Japan.

0556-2813/95/51(1)/178(4)/$06.00

projectiles emerged from the production targets at laboratory angles between 3° and 8° and, due to the solenoid's angular magnification, reached the secondary target traveling at angles between 1° and 2.7° to the axis of the system.

The secondary targets were 0.9 mg/cm^2 ^{12}C, 1.0 mg/cm^2 ^{nat}Ni, and 0.5 mg/cm^2 ^{197}Au, in which the incident particles lost 0.6, 0.4, and 0.1 MeV, respectively.

Scattered particles were detected and identified by a Si telescope having a 22-μm transmission counter, 300 mm^2 in area and 12.1 cm from the target, and a 160-μm stopping detector with lateral dimensions 25 mm×25 mm. The conical beam, and large detectors required by the small beam intensity, lead to relatively large angular acceptance. A typical case is ^{6}He+^{12}C at 30° lab (44.5° c.m.) where the rms angular deviation in the c.m. system is 3.8°.

The secondary beam included about eight times as many 15.3-MeV α particles from the ^{9}Be(^{7}Li,^{5}He)^{11}B reaction as ^{6}He projectiles. The intensity ratio I_4/I_6 of these two components was in fact constant in time. The strongest evidence for this is that repeated measurements, for the same target at the same angle, gave statistically consistent ratios S_4/S_6 (where S_i particles of type i are elastically scattered) even when they were days apart and had high statistical accuracy. Examples are given in Table I. Thus, the α particles were useful for experimental tests and normalized purposes, as we later explain.

III. DATA ANALYSIS

Measurements with the ^{197}Au target were made at laboratory angles between 15° and 55°. For the α particles, σ/σ_R (the ratio of the elastic differential cross section to that for Rutherford scattering) is exactly 1, since 25-MeV α+Au elastic scattering [8] follows the Rutherford law to at least 60°. We can therefore determine σ/σ_R for ^{6}He from the equation

$$(\sigma/\sigma_R)_6 = \frac{S_6}{S_4}\frac{I_4}{I_6}\frac{E_6^2}{E_4^2}\frac{J_6 \sin^4(\theta_6/2)}{J_4 \sin^4(\theta_4/2)} , \qquad (1)$$

where J_i is the c.m.-to-lab transformation coefficient, E_i is the c.m. energy, and θ_i is the c.m. scattering angle for particles of type i. We take a cross-section-weighted average of J, E, and $\sin^4\theta$ over the beam directions and detector area. We determine the beam intensity ratio to be 8.37±0.38 by assuming $(\sigma/\sigma_R)_6$ to be exactly 1 at 15° lab. The cross sections at larger angles are then found

TABLE I. The ratio S_4/S_6 of ^{4}He and ^{6}He elastically scattered at 15° lab.

Run	Target	Date	S_4/S_6
75	C	6/19/92	3.72±0.13
97	C	6/21/92	3.61±0.12
74	Ni	6/19/92	3.45±0.04
99	Ni	6/21/92	3.41±0.03
106	Ni	6/21/92	3.40±0.02

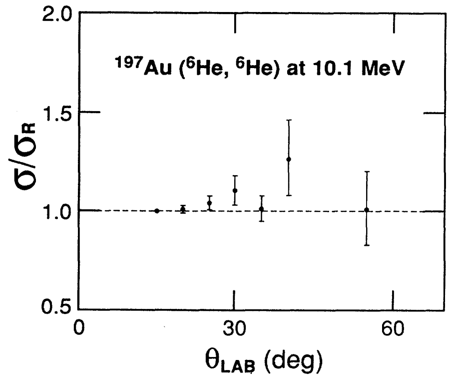

FIG. 1. The ratio of the elastic-scattering cross section for 10.1-MeV ^{6}He on ^{197}Au to Rutherford scattering, as determined from Eq. (1).

and displayed in Fig. 1; they are consistent with pure Rutherford scattering with $\chi^2/N = 0.9$. One could instead assume Rutherford scattering for ^{6}He and consider these data a test of the experiment.

We determined the ^{6}He+Ni elastic cross section from (a) the elastic-scattering ratio S_6/S_4, and (b) optical-model calculations for α+Ni. This is necessary since the incident flux is too small to measure with a Faraday cup, which in any case would also count the beam contaminants. Good optical-model fits to α+^{58}Ni elastic-scattering data exist at both 10.1 and 16.1 MeV [9,10]. We interpolated between calculations for these energies to find the cross section at 15.3 MeV, the α energy focused by the solenoid. This interpolation is reasonable considering the statistical uncertainty of our data; for example, at 45° lab the 10.1- and 16.1-MeV ratios-to-Rutherford are 0.64 and 0.73, respectively. The result-

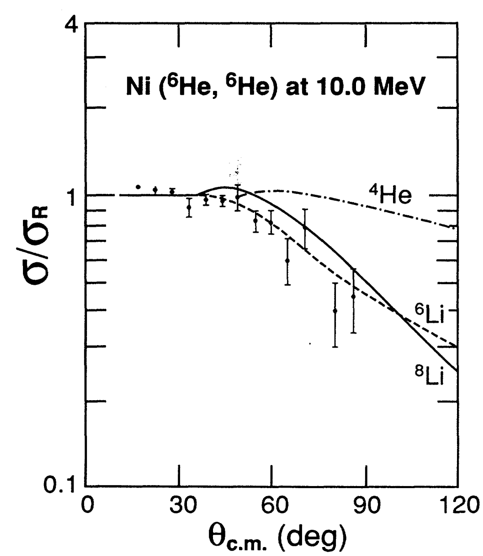

FIG. 2. Elastic scattering of 10.0-MeV ^{6}He from ^{nat}Ni. The curves show optical-model predictions, using parameters shown in Table II. Symbols near the curves identify the projectile for which each OMP parameter set was first used.

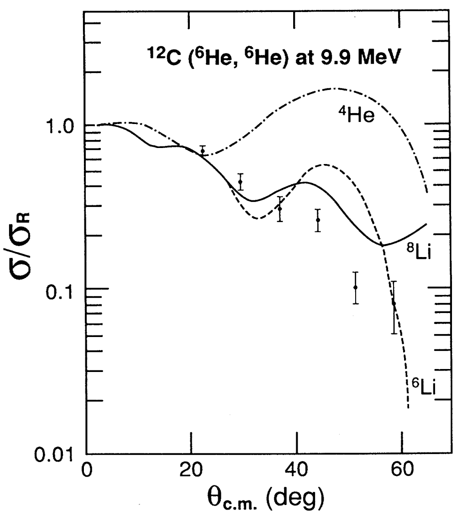

FIG. 3. Elastic scattering of 9.9-MeV ^{6}He from ^{12}C, similar to Fig. 2. The data were normalized to fit the ^{6}Li and ^{8}Li optical-model predictions at the smallest angle.

ing angular distribution, expressed as σ/σ_R, is shown in Fig. 2. Here, again, we have allowed for the difference between α and ^{6}He c.m. scattering angles and energies, and have averaged the Rutherford cross section over beam directions and detector area.

Normalization of the ^{6}He+^{12}C data to the elastic α yield was however unsuitable since (a) the α-^{12}C elastic cross section [9,11–13] varies rapidly with both angle and energy, and (b) the α-^{12}C optical-model fits are of variable quality. For example, predictions of σ/σ_R for 15.3 MeV α's at 15° lab varied from 0.75 to 1.3 for various OMP sets [9,11,13] used to fit 9–18-MeV α-^{12}C data. The ^{12}C data were therefore normalized to counts by a fixed detector located at 30° in the second scattering chamber. This number, in turn, was compared with the product of running time and current on the accelerator's high-energy shutter. The ratio of these two quantities usually remained within ±8% of its average value; runs showing larger fluctuations were discarded. The ^{6}He+^{12}C elastic-scattering data are presented in Fig. 3, where the error bars include statistical uncertainties and the ±8% monitoring uncertainty added in quadrature. All data were renormalized by a common factor so that the smallest-angle datum fitted two of the optical-model predictions.

IV. OPTICAL-MODEL PREDICTIONS

Figures 2 and 3 show predictions from various optical-model parameter (OMP) sets for comparison with our data. The parameters are listed in Table II. The calculations, which employed the code SNOOOPY8Q, assumed a standard Woods-Saxon six-parameter nuclear potential with volume absorption and without spin-orbit coupling, and the Coulomb potential of a uniformly charged sphere. They were done at the target-center energies of 9.9 and 10.0 MeV for the ^{12}C and Ni targets, respectively.

The ^{6}He+Ni data (Fig. 2) show a clear preference for the ^{6}Li and ^{8}Li OMP's over these for ^{4}He. This is expected, especially for ^{6}Li, which resembles ^{6}He in both structure and binding much more than the α particle does. The ^{6}Li and ^{8}Li parameters [15,2] were derived from 12- and 14-MeV data, respectively. We did other calculations (not shown) using OMP's from 51- and 210-MeV ^{6}Li data [16,17]; these predictions dropped less rapidly with increasing angle than those shown, and therefore fitted the data less well.

For ^{12}C (Fig. 3), as for Ni, the ^{4}He OMP fails to predict the decrease with angle of the cross section. (Another OMP set for 9.3 MeV α+^{12}C, with real potential depth 149 MeV [7], shows a deep minimum at 45°, but rises to a still greater maximum beyond 60°.) The ^{6}Li and ^{8}Li predictions drop at large angles but seem to show more oscillations from the data. Holding other parameters of the ^{8}Li OMP fixed, we made a limited but unsuccessful search for imaginary potential depths and radii which would reduce the oscillations.

The ^{6}Li OM fit shown in Fig. 3 uses one [14] of two energy-dependent ^{6}Li+^{12}C OMP sets [14,18] which have been reported. Their primary difference is that Vineyard *et al.* [14] use a volume imaginary potential while Poling *et al.* [18] use surface absorption; the two studies fit available data from 4.5 to 156 MeV, and from 4.5 to 63 MeV, respectively. The fit shown in Fig. 3 was judged marginally better than that obtained with the Poling OMP since, for the latter, σ/σ_R rises to 0.61 at 46° vs 0.55 for the displayed curve. Otherwise, the two fits are nearly indistinguishable throughout the range of our data. Still other calculations (not shown) using ^{6}Li OMP's [16,17] with deep imaginary potential ($W \simeq 30$ MeV) gave predictions very similar to that for ^{8}Li.

The findings that ^{4}He OMP's are unsuitable for ^{6}He, and that those for ^{6}Li work better, are not surprising when we consider the binding and structure of these

TABLE II. Optical-model potentials for ^{6}He elastic scattering. The first two columns name the target nucleus in the present study, and the projectile for which an OM set was originally used, respectively. We use the convention $R = r_0 A_t^{1/3}$.

Target	Origin	V (MeV)	r_{0r} (fm)	a_r (fm)	W (MeV)	r_{0i} (fm)	a_i (fm)	r_{0c} (fm)	Ref.
^{12}C	^{4}He	88.6	1.42	0.39	0.22	1.42	0.39	1.30	[9]
^{12}C	^{6}Li	171.5	1.26	0.79	3.63	2.40	0.62	2.24	[14]
^{12}C	^{8}Li	175.0	1.30	0.80	15.10	2.25	0.80	2.44	[2]
Ni	^{4}He	165.0	1.62	0.40	11.40	1.62	0.40	1.30	[9]
Ni	^{6}Li	152.0	1.39	0.75	6.32	2.33	0.61	1.44	[15]
Ni	^{8}Li	175.0	1.30	0.80	4.00	2.25	0.80	1.97	[2]

three nuclei. It would however be useful to have accurate OMP's specifically for ^{6}He. We know that those for ^{6}Li are not fully satisfactory for ^{6}He, yet they must sometimes be used in DWBA calculations of reactions producing ^{6}He in the exit channel, such as [19] ^{6}Li(^{6}Li,^{6}He)^{6}Be.

V. CONCLUSIONS

10-MeV ^{6}He projectiles undergo pure Rutherford scattering from a ^{197}Au target, but have elastic cross sections well below Rutherford scattering at angles greater than about 20° c.m. for ^{12}C and 50° for Ni. Optical-model calculations fit the angular distributions much better when parameters first obtained for ^{6}Li or ^{8}Li rather than ^{4}He are used. However the ^{6}He+^{12}C data fall more steeply with increasing angle, and oscillate less, than the OM calculations.

More comprehensive and accurate ^{6}He elastic-scattering data are needed to further constrain the optical-model parameters. Improved parameters are needed for both a better understanding of the ^{6}He-nucleus interaction and more realistic DWBA calculations of nucleon transfer and charge exchange reactions, such as (^{7}Li,^{6}He) and (^{6}Li,^{6}He).

ACKNOWLEDGMENTS

We thank E. Berners and J. Kaiser for assistance with the tandem accelerator and the Notre Dame on-line computer, J. Bajema for assistance with the University of Michigan data-analysis computer, and P. Schwandt for giving us his optical-model code SNOOPY8Q. The National Science Foundation supported this work under Grants PHY-91-22067, PHY-92-08468, PHY-92-14992, and PHY-91-00708. Daniel Butts's participation was supported by NSF-REU Grant PHY-90-00713 to the University of Notre Dame, and Jonathan Fetter's by a grant from the Oberlin College Research and Development Committee.

[1] C.-B. Moon *et al.*, Phys. Lett. B **297**, 39 (1992).
[2] F. D. Becchetti *et al.*, Phys. Rev. C **48**, 308 (1993).
[3] I. Tanihata, D. Hirata, T. Kobayashi, S. Shinoura, K. Sugimoto, and H. Toki, Phys. Lett. B **289**, 261 (1992).
[4] A. Csoto, Phys. Rev. C **48**, 165 (1993).
[5] R. J. Smith, J. J. Kolata, K. Lamkin, A. Morsad, K. Ashktorab, F. D. Becchetti, J. A. Brown, J. W. Jänecke, W. Z. Liu, and D. A. Roberts, Phys. Rev. C **43**, 761 (1991).
[6] W. Z. Liu, Ph.D. thesis, University of Michigan, 1990 (unpublished).
[7] J. J. Kolata, A. Morsad, X. J. Kong, R. E. Warner, F. D. Becchetti, W. Z. Liu, D. A. Roberts, and J. W. Jänecke, Nucl. Instrum. Methods B **40/41**, 503 (1989).
[8] L. McFadden and G. R. Satchler, Nucl. Phys. **A84**, 177 (1966).
[9] F. P. Brady, J. R. Jungerman, and J. C. Young, Nucl. Phys. **A98**, 241 (1967).
[10] W. C. Hermans, H. R. E. Tjin A Djie, L. D. Tolsma, and B. J. Verhaar, Nucl. Phys. **A141**, 431 (1970).
[11] E. B. Carter, G. E. Mitchell, and R. H. Davis, Phys. Rev. **133**, B1421 (1964).
[12] L. L. Ames, Phys. Rev. C **25**, 729 (1982).
[13] D. R. Ober and O. E. Johnson, Phys. Rev. **170**, 924 (1968).
[14] M. F. Vineyard, J. Cook, K. W. Kemper, and M. N. Stephens, Phys. Rev. C **30**, 916 (1984).
[15] K. O. Pfeiffer, E. Speth, and K. Bethge, Nucl. Phys. **A206**, 545 (1973).
[16] L. T. Chua, F. D. Becchetti, J. Jänecke, and F. L. Milder, Nucl. Phys. **A273**, 243 (1976).
[17] A. Nadasen, M. McMaster, G. Gunderson, A. Judd, S. Villaneuva, P. Schwandt, J. S. Winfield, J. van der Plicht, R. E. Warner, F. D. Becchetti, and J. W. Jäneke, Phys. Rev. C **37**, 132 (1988).
[18] J. E. Poling, E. Norbeck, and R. R. Carlson, Phys. Rev. C **13**, 648 (1976).
[19] W. R. Wharton, Phys. Rev. C **9**, 164 (1974).